Utilization of cellulose and ulvan from the green seaweed *Ulva lactuca* in the development of composite edible films with natural antioxidant properties

Mohamed Gomaa[1] · Arwa A. Al-Badaani[1] · Awatief F. Hifney[1] · Mahmoud S. Adam[1]

Abstract

Cellulose and ulvan were extracted sequentially from the green seaweed *Ulva lactuca* and were used for the development of edible films with natural antioxidant properties. The composite films were composed of cellulose, polyvinyl alcohol, glycerol as plasticizer and different ulvan concentrations. The interaction between ulvan and film components was described by FT-IR analysis, which confirmed the formation of hydrogen bonding interactions between cellulose and ulvan. The incorporation of ulvan into the cellulose films markedly increased film thickness, water solubility and water vapor permeability, whereas the oxygen permeability was decreased. Additionally, the composite films showed good barrier properties against UV and visible light. The moisture sorption of the films was modelized using Peleg's model which exhibited a satisfactory fitting to the experimental data. The thermal stability was markedly enhanced in the presence of high concentration of ulvan. Furthermore, the incorporation of ulvan to cellulose films enhanced its antioxidant properties as measured by total antioxidant assay (TAC), ferric reducing antioxidant power (FRAP), hydroxyl radical scavenging activity (HRSA) and iron chelating activity (ICA). The use of water and 3% acetic acid as food simulants indicated that the FRAP was higher in case of water, while the opposite trend was observed for the HRSA and ICA. Overall, the developed cellulose/ulvan films could have potential uses in food packaging to promote the shelf-life of different food products.

Introduction

There is a growing demand for the development of films and coatings from renewable, eco-friendly and low-cost natural resources to substitute synthetic petroleum-based plastics and reduce their accumulation in the environment. These films and coatings are generally regard as safe and more importantly they are biodegradable and can be used for food and non-food packaging applications. The use of edible films plays an important role in extending the shelf life of food products by preventing moisture loss, light deterioration, oxidative rancidity and microbial spoilage (Razavi et al. 2015; Tavassoli-Kafrani et al. 2016).

Generally, different biopolymers such as polysaccharides, proteins and lipids can be used for the development of films and coatings. Within this prospect, alginate, carrageenan and agar are the most exploited algal polysaccharides in the preparation of edible films compared to other algae-derived polymers such as cellulose, ulvan and starch. (Gomaa et al. 2018; Guidara et al. 2019, 2020). These edible and biodegradable films can be utilized to restrain the movement of water, oxygen, and carbon dioxide as well as they can enhance selected nutritional properties (Bhattacharya and Kandeepan 2017).

Currently algal biomass is considered as a promising alternative for cellulose production since it can be cultivated in several aquatic media without the need for soil, fertilizers and freshwater and cannot interfere with any food resource (Jmel et al. 2016). In addition, the rapid growth of the algae allows fast harvesting of the algal biomass compared with terrestrial plants. Generally, cellulose extracted from algae is characterized by small and thin fibers which have a larger surface area and smaller particle size than plant-derived cellulose

✉ Mohamed Gomaa
m_gomaa@aun.edu.eg

[1] Botany & Microbiology Department, Faculty of Science, Assiut University, Assiut 71516, Egypt

(Bogolitsyn et al. 2020). However, there is little information available in the literature regarding the utilization of algal cellulose in the development of edible films compared to plant-derived cellulose (Zanchetta et al. 2021). El Achaby et al. (2018) prepared nanocomposite films based on cellulose nanocrystals (CNCs) derived from red algal waste and polyvinyl alcohol. In another study, CNCs were prepared from the cellulose extract from the green macroalga *Ulva* (*Enteromorpha*) *prolifera* and used these for the preparation of composite films using the water-soluble polysaccharides isolated from the same seaweed. Sucaldito and Camacho (2017) incorporated CNCs derived from the green alga *Cladophora rupestris* into starch films to promote their mechanical properties. However, pristine cellulose lacks adequate antimicrobial and antioxidant properties which are important in active food packaging (Valizadeh et al. 2019; Pirsa et al. 2020). Therefore, the development of bioactive composite films based on cellulose has been considered in recent studies (Valizadeh et al. 2019).

Ulva species represent an industrially important biomass which is found in enormous quantities almost all over the world. This seaweed is rich in polysaccharides such as cellulose and ulvan. Ulvan is a water-soluble sulphated polysaccharide mainly composed of rhamnose and uronic acids (Kidgell et al. 2019). Ulvan can be used in various fields, from food supplements to biomedical applications (Guidara et al. 2020). Generally, there have been few attempts regarding the use of ulvan in the preparation of edible films. Guidara et al. (2019, 2020) extracted ulvan from *Ulva lactuca* and evaluated the role of extraction condition on the development of ulvan-based films. In another study, ulvan from *Ulva fasciata* and semi-refined carrageenan from *Kappaphycus alvarezii* were used for the preparation of antioxidant films suitable for food packaging (Ganesan et al. 2018). To the best of our knowledge, no attempts have been carried out to utilize algal cellulose and ulvan in the development of edible films with natural antioxidant properties. Therefore, the present study aimed to develop antioxidant-edible films based on cellulose and ulvan extracted from the same biomass of the green seaweed *U. lactuca*. Furthermore, the study investigated the effect of different ulvan concentrations on the physicochemical and antioxidant properties of the developed films.

Materials and methods

Seaweed sample and sequential extraction of cellulose and ulvan based on a biorefinery concept

The biomass of the green alga *Ulva lactuca* L. was collected from the supralittoral zone of Alexandria, Egypt (N 16º31' E 30º0') during winter.

The *U. lactuca* biomass was air-dried and milled using a home blender and various components were extracted under a biorefinery concept. Firstly, starch and lipid were removed from the dried biomass as described previously (Prabhu et al. 2019). Then, ammonium oxalate aqueous solution (0.02% w/v) was used to isolate ulvan at 85 °C for 1 h (Kidgell et al. 2019). The residual biomass was collected by filtration, washed several times using distilled water and was used for cellulose extraction. Ulvan in the filtrate was separated by ethanol precipitation, left overnight at 4 °C, collected by centrifugation (4800 x*g*, 10 min), and oven dried (80 °C). Cellulose was isolated after alkali treatment and bleaching of the residual biomass. The conditions for the alkali treatment step were: sodium hydroxide 5% (w/v), temperature 100 ºC and time 2 h. Bleaching was performed using acetic acid/NaClO$_2$ aqueous mixture (5%/2%) (v/v), temperature, 60 °C and time, 1 h. The collected residue was then treated with hydrochloric acid (5% v/v) and left in a boiling water bath for 5 min. The extracted cellulose was washed until neutrality and finally dried at 60 °C. The molecular weight of cellulose was determined by an Ubbelohde capillary viscometer at 25 °C (Zhou et al. 2004), and the crystallinity was estimated based on FT-IR analysis as reported previously (Lee et al. 2015; Gomaa et al. 2021). The total sugar contents of ulvan was estimated by the UV-sulfuric acid method (Albalasmeh et al. 2013). Sulphate content in ulvan was determined by using the BaCl$_2$-gelatin turbidity method (Bhadja et al. 2016) and uronic acid content was determined based on the method of Bitter (1962). Folin–Ciocalteu reagent was used to determine the total phenolic contents of the crude ulvan extract (Lister and Wilson 2001), while the protein contents were measured according to the method of Lowry et al. (1951). The molecular weight of the extracted ulvan was determined using capillary viscometry and Mark-Houwink equation as described by Ganesan et al. (2018).

Preparation of cellulose and cellulose/ulvan films

Cellulose (5 g dry wt.) was dissolved in 100 mL of NaOH/urea aqueous solution (7/12 wt%) and left for 24 h at 4 °C (Qi et al. 2008). After vigorous shaking, acetic acid (4% v/v) was added until the cellulose was precipitated. Then, cellulose was collected by centrifugation and washed several times with distilled water until neutrality. The regenerated algal cellulose was finally suspended in distilled water to a final concentration of 5% (w/v). Polyvinyl alcohol (PVA) (5% w/v) was dissolved in distilled water at 60 °C. Cellulose films were prepared by mixing 5 mL of the regenerated cellulose and 5 mL of PVA, and the mixture was homogenized for 1 h at 250 rpm. PVA

was incorporated to the films to increase their flexibility and toughness (Xie et al. 2022). For the preparation of cellulose-ulvan films, ulvan was mixed with the cellulose-PVA solution to obtain a final ulvan concentration of 0.12, 0.24, or 0.48 g g^{-1} cellulose. Then glycerol was added as a plasticizer (0.3 g g^{-1} cellulose) and the film forming solutions were further homogenized for 1 h. Ten milliliter of the film forming mixtures was poured into a polyethylene Petri dish and left to dry at 40 ºC. Finally the intact film was peeled off and kept in a desiccator at 25 °C for 48 h until further analysis. The developed films were designated as C, C/0.12U, C/0.24U, and C/0.48U based on the ulvan concentration as 0, 0.12, 0.24, and 0.48 g g^{-1} cellulose, respectively.

Film analysis

Fourier transform infrared spectroscopy (FT-IR)

FT-IR spectra of the films was recorded using Nicolet IS 10 FT-IR spectrophotometer in the 4500—500 cm^{-1} wavelength range.

Film thickness and density

Film thickness was evaluated by using a manual micrometer with an accuracy of ± 0.01 mm. For each film, 10 measurements were taken randomly. The weight of film pieces (1×1 cm) was measured and film density was expressed as the ratio of film mass to its volume (the product of area and thickness).

Film color, light transmittance and opacity

Film color was determined as described by Razavi et al. (2015). The light transmittance of the films was recorded at 200, 280, 400, 600 nm against air as a blank in a UV−vis spectrophotometer. The opacity of the film (UA mm^{-1}) was calculated by dividing the absorbance value at 280 or 600 nm by the film thickness (mm).

Water solubility

The water solubility was measured as described by Syarifuddin et al. (2019). The films were dried at 90 ºC for 24 h. Then film pieces were immersed in 20 mL distilled water at 25 ºC without agitation. After 24 h, the insoluble film fraction was collected by centrifugation (6000 rpm, 5 min) and oven dried (105 ºC, 24 h). The water solubility (WS %) was calculated using the following equation:

$$Water\ solubility(\%) = \frac{Initial\ \mathrm{dry\ weight} - Final\ dry\ weight}{Initial\ dry\ weight} \times 100 \tag{1}$$

Water vapor permeability (WVP)

The water vapor permeability (WVP) of the films was determined according to the method of (Zhang et al. 2016). The film samples were cut and fixed with elastics at the top of a weighing bottle which contained anhydrous CaCl$_2$ (5.0 g). All the bottles were then placed into a desiccator containing NaCl saturated solution (75% RH) at 25 ºC. The weight change of the bottles was determined at 1 h intervals and over a 7 h period. The water vapor transmission rate per unit area (WVTR, g s^{-1} m^{-2}), and WVP (g mm m^{-2} s^{-1} Pa^{-1}) were calculated using the following equations:

$$WVTR = K/A \tag{2}$$

$$WVP = WVTR \times D/\Delta P \tag{3}$$

Where K (g s^{-1}) is the slope obtained by linear regression analysis of the plot between weight of the moisture gain (g) and time (t, s^{-1}), A is the area of the exposed film surface (m), D is the average film thickness (mm), and ΔP is the water vapor pressure difference between the two sides of the film.

Oxygen permeability

Oxygen permeability (OP) of the films was determined as reported by Zhang et al. (2016). The deoxidizing reagent was prepared by mixing reduced iron powder, NaCl, and activated carbon in a proportion of 0.5: 1.5: 1.0 g in a weighing bottle. The bottles were covered by the film samples (pre-equilibrated at 90% RH in a desiccator with saturated BaCl$_2$ in its bottom) and fixed with elastics. The bottles were preserved at 90% RH for 48 h at 25 ºC. The OP was calculated using Eq. (4), and was converted into a normalized constant film thickness, d, of 100 μm (OP$_{100}$) using Eq. (5) (Jost et al. 2014).

$$OP = (W_f - W_i)/(t \times A) \tag{4}$$

$$OP_{100} = OP \times (\frac{d}{100}) \tag{5}$$

Where W_f is the final weight of the weighing bottle after 48 h; W_i is the initial weight of the weighing bottle; t is time (s), and A is the area of the exposed film surface (m^2).

Moisture sorption

The films were dried to a constant weight at 90 ºC and placed in a desiccator maintained at 75% RH and 25 ºC. The changes

in the weight of the films were determined at regular time intervals and the moisture content (M_t) of the films as a function of time was determined using Eq. (6):

$$M_t\% = [(W_t - W_0)/W_0] \times 100 \tag{6}$$

Where W_0 is the initial dry weight of the film sample, and W_t is the weight of the film sample at fixed time (t). Peleg's equation model was used to analyze the moisture sorption, the design was based on Peleg's equation (Peleg 1988):

$$M_t = M_0 + [t/(K_1/K_2 t)] \tag{7}$$

M_t represents the moisture content after time t, and M_0 is the initial moisture ($M_0 = 0$). The constants K_1 and K_2 are the Peleg's rate constant and Peleg's capacity constant, respectively. The Peleg's rate constant, K_1, relates to the initial mass change (R_0) of any component:

$$R_0 = {}^1/_{K_1} \tag{8}$$

While the Peleg's capacity constant, K_2, relates to the contents at equilibrium (M_∞): the maximum attainable moisture content

$$M_\infty = M_0 + ({}^1/_{K_2}) \tag{9}$$

The linear relationship of Eq. (7) is:

$$t/(M_t - M_0) = K_1 + K_2 t \tag{10}$$

The linear regression analysis of the relationship between $t/(M_t - M_0)$ vs. t offers a simple way to calculate K_1 and K_2.

Thermal gravimetric analysis (TGA)

The thermal stability of the developed films was performed using a DTG-60H analyzer. from 15 to 500 °C in an inert nitrogen atmosphere with a flow of 40 mL min^{-1} and a heating rate of 10 °C min^{-1}.

Antioxidant activity

Two different solvents viz. water and acetic acid (3%) were used as simulants for aqueous and acidic food products, respectively. Film samples (50 mg) were dissolved for 24 h at 25 °C in 10 mL solvent, then aliquots of the dissolved samples were used for the measurement of antioxidant activities.

Total antioxidant capacity (TAC)

The total antioxidant activity of the developed films was evaluated by the phosphomolybdenum method (Prieto et al. 1999). An 0.1 mL sample aliquot was mixed with 3.0 mL reagent solution (0.6 M sulfuric acid, 28 mM sodium phosphate and 4 mM ammonium molybdate) and incubated at 95 °C for 90 min in a water bath. The absorbance was measured at 695 nm against a suitable blank. Total antioxidant activity was expressed as the number of grams equivalent to ascorbic acid (μg AAEq g^{-1} film).

Ferric reducing antioxidant power

The ferric reducing power was determined by the method described by Ferreira et al. (2007). A 0.125 mL sample aliquot was mixed with 0.125 mL phosphate butter (0.1 M, pH 7) and 0.125 mL potassium ferricyanide (1% w/v). The mixture was incubated at 50 °C for 20 min, then the reaction was terminated by the addition of 0.125 mL of trichloroacetic acid (10% w/v). The solution was then mixed with 0.5 mL distilled water and 0.1 mL of ferric chloride (0.1% w/v) and the absorbance was measured at 700 nm. The FRAP values were determined against an ascorbic acid calibration curve and expressed as μg equivalents of ascorbic acid per gram of film.

Hydroxyl radical scavenging activity

Hydroxyl radical scavenging activity (HRSA) was estimated according to Zhong et al. (2010). Hydroxyl radicals were generated from $FeSO_4$ and detected by their ability to hydroxylate salicylate. To a 0.1 mL of sample, 1 mL of $FeSO_4$ (9 mM), 1 mL H_2O_2 (0.3%), and 0.5 mL of salicylic acid–ethanol solution (5 mM) was added. The reaction mixture was incubated in a water bath at 37 °C for 30 min. Then the mixture was completed to 5 mL using distilled water. The absorbance was measured at 510 nm and ascorbic acid was used as the positive control. The HRSA was calculated as follows:

$$HRSA(\%) = (\{A_0 - (A_1 - A_2)\}) \times 100 \tag{11}$$

Where A_1 is the absorbance of the sample or ascorbic acid, and A_0 is the absorbance of the control (without sample or ascorbic acid), A_2 is the absorbance of the reagent blank without salicylic acid.

Iron chelation assay

The ability of the films to chelate Fe (II) was estimated as described by (Puntel et al. 2005). A 100 μL samples was mixed with 336 μL of tris–HCl buffer (0.1 M, pH 7.4) and $FeSO_4$ (300 μL, 2 mM). After 5 min, 26 μL of 1,10 phenathroline (0.25% w/v) was added and the absorbance was measured at 510 nm. The Fe^{+2} chelating ability was calculated as:

$$Fe^{+2} \text{chelating ability } (\%) = (A_C - A_S)/A_C \times 100 \tag{12}$$

Whereas A_S and A_C is absorbance of the sample and the control, respectively.

Statistical analysis

The statistical analysis used Microsoft Windows Excel 2019 and SPSS program (IBM SPSS Statistics for Windows, Version 21.0; IBM Corp., USA). Triplicate experiments were used in the analysis, except in the determination of film thickness, density, and color where 10-measurements were used. Data were subjected to analysis of variance (ANOVA) and multiple range checks of the Duncan test were used to assess the significant variation at $p < 0.05$.

Results

The green seaweed *U. lactuca* was utilized as a natural, safe, and renewable resource for cellulose and ulvan for the development of edible films. Under the extraction conditions, the cellulose yield was $5.50 \pm 0.44\%$ and was characterized by a molecular weight of 2.53 ± 0.25 kDa and a crystallinity of $93.47 \pm 1.25\%$. The ulvan yield was $10.97 \pm 1.33\%$ and its total sugar, uronic acid, sulfate, protein and phenolic contents were $24.69 \pm 5.0\%$, $36.12 \pm 1.42\%$, 17.78 ± 0.77, 0.63 ± 0.078, and $1.58 \pm 0.18\%$ (w/w), respectively. The molecular weight of the extracted ulvan was 327.44 ± 9.66 kDa (as determined by Mark-Houwink equation). The developed films were easily manageable, easily detachable, without bubbles, and were non-steaky in nature (Fig. 1).

Fourier transform infrared spectroscopy (FT-IR)

The FT-IR spectra of cellulose extracted from *U. lactuca* have been published previously (Gomaa et al. 2021). The characteristic FT-IR spectrum of ulvan is depicted in Fig. 2a. The bands at 3397 cm^{-1} are attributed to the stretching vibrations of the hydroxyl group (O–H) characteristic to saccharide structures. Absorption peaks at 1663 cm^{-1} indicate the asymmetric bending vibration of the carboxylate group (C=O) of uronic acids in ulvan (Hussein et al. 2015) and at 1637 cm^{-1} relate to bending of water overlapped with

symmetric stretching vibration of COO$^-$ (Zhong et al. 2010). Bands of absorption spectra at 1373 cm^{-1} are attributed to asymmetric stretching of sulfate groups. Furthermore, the band at 1316 and 1097 cm^{-1} for ulvan corresponds to the symmetric and asymmetric stretching vibrations of the $RO-SO_3^{-}$ bond of the sulphate groups (Fernando et al. 2017). The band at 830 cm^{-1} derived from the bending vibration of $C-O-S$ of sulfate in equatorial position and further confirms the existence of sulphate groups in the ulvan extract (Hung et al. 2021).
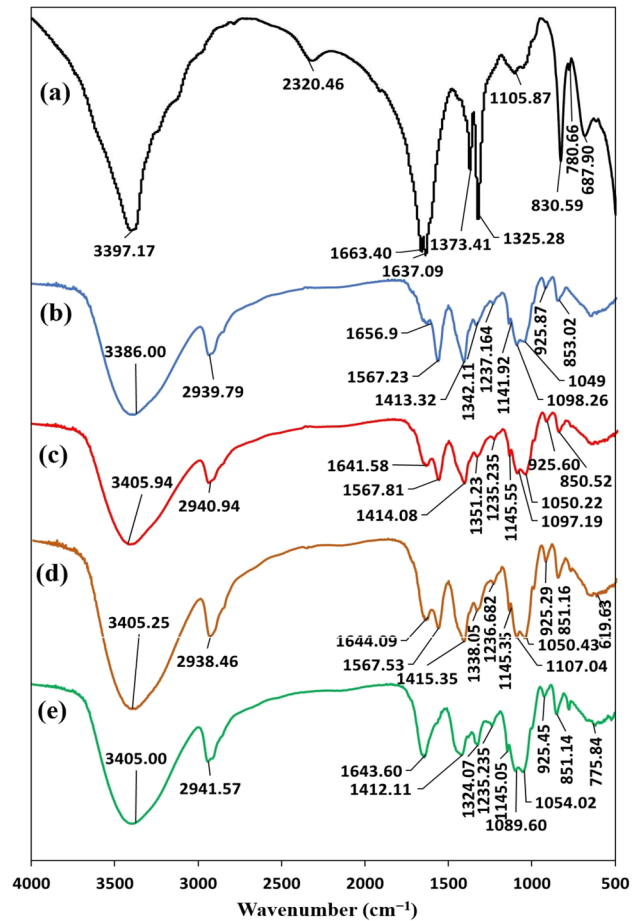

Fig. 2 FTIR spectra. (**a**) Ulvan extract, (**b**) Cellulose film, (**c**) Cellulose/0.12 Ulvan, (**d**) Cellulose/0.24 Ulvan and (**e**) Cellulose/0.48 Ulvan film
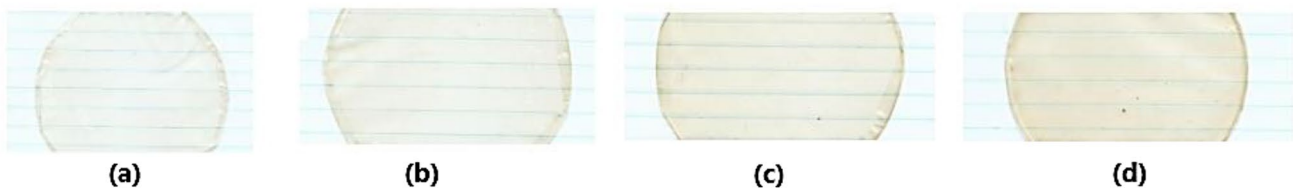

Fig. 1 Optical images of the developed films. (**a**) Cellulose, (**b**) Cellulose/0.12 Ulvan, (**c**) Cellulose/0.24 Ulvan (**d**) Cellulose/0.48 Ulvan

The FT-IR spectra of the developed films were analyzed to determine the specific interactions between cellulose and ulvan (Fig. 2). The $-OH$ stretching vibrations band was shifted to a higher wave number (~ 3405 cm^{-1}, Fig. 2c,d,e) in the cellulose/ulvan films, reflecting the existence of more hydrogen bonding between cellulose and ulvan in the composite films compared to C film (~ 3386 cm^{-1}) (Fig. 2b). The asymmetric bending vibration of the carboxylate group ($C=O$) was observed at ~ 1656 cm^{-1} in the C film. This band was shifted to a lower wavenumber ($1641 - 1644$ cm^{-1}) in the composite films, which may be related to the interaction between cellulose and ulvan molecules. Furthermore, the absorption band for stretching vibration of the carboxylate anion ($O=C-O^-$) centered at ~ 1567 cm^{-1} in ulvan was markedly reduced in the C/0.12U and C/0.24U films, and completely disappeared in the C/0.48U film. This observation indicates the interaction between ulvan and cellulose through the carboxylate groups and the interaction was increased by increasing ulvan concentrations. The band observed at ~ 1342 cm^{-1} in the C film was attributed to the OH plane deformation vibration and exhibited a marked shift in the composite films (Schwanninger et al. 2004). Furthermore, the C–O–C linkages of cellulose in C film at ~ 1141 cm^{-1} were slightly shifted to a higher wavenumber (~ 1145 cm^{-1}) in the composite films.

Film thickness and density

Thickness of the edible films is one of the most crucial characteristics that affects its properties such as mechanical, barrier, and water vapor permeability (Galus and Lenart 2013). The thickness of the developed films ranged between 0.068 and 0.083 mm, with a significant ($p < 0.05$) increase in film thickness with the incorporation of ulvan (Table 1). In addition, increasing ulvan concentration in the films exhibited significant effects on film thickness at high concentrations (C/0.24U and C/0.48U films). Additionally, the incorporation of ulvan to the films showed negligible effects on the density of the developed films in comparison to the C film (Table 1).

Optical properties

The results of the film color parameters are listed in Table 1. All the developed films were characterized by high L^* and b^*, while a^* values were low. The light transmission of the films was measured in the UV range (200 and 280 nm) and visible region (400 and 600 nm) and the values of light transmission at 600 nm was used to calculate the film opacity (Table 1). At 200 nm all the developed films exhibited no light transmission providing an effective UV barrier. While at 280 nm, the light transmittance reached 9.93% for cellulose (C) film. This value was significantly reduced in the

Table 1 Thickness, color parameters, light transmission, and opacity of the developed films from cellulose and ulvan from *U. lactuca*

Film type	Thickness (mm)	Density (g cm^{-3})	Light transmission (%)				Color parameters			Opacity (UA mm^{-1})	
			T_{200}	T_{280}	T_{400}	T_{600}	L^*	b^*	a^*	280 nm	600 nm
C	0.068±0.004[a]	0.129±0.005[a]	0.00	9.93±1.43[d]	40.33±5.35[d]	57.80±2.72[b]	96.33±0.86[c]	0.90±0.11[a]	-2.17±0.85[b]	14.83±1.55[a]	3.50±0.33[ab]
C/0.12U	0.079±0.005[b]	0.141±0.012[a]	0.00	4.25±0.06[c]	34.85±1.11[c]	59.45±0.19[b]	94.49±0.85[b]	2.29±0.34[b]	-2.55±0.72[a]	17.28±0.32[b]	2.85±0.07[a]
C/0.24U	0.083±0.003[c]	0.123±0.002[a]	0.00	1.75±0.17[b]	28.1±1.13[b]	55.30±1.73[b]	92.65±1.07[a]	4.46±0.21[c]	-2.31±1.00[b]	21.16±0.52[c]	3.09±0.09[a]
C/0.48U	0.083±0.004[c]	0.128±0.003[a]	0.00	0.25±0.06[a]	19.78±2.73[a]	44.75±4.52[a]	92.13±1.14[a]	7.33±0.08[d]	-2.56±1.03[a]	31.30±1.39[d]	4.20±0.47[b]

All values are mean ± standard deviation

Different letters in the same column indicate significant difference among different films ($p < 0.05$)

biocomposite cellulose-ulvan films and the reduction was dependent on ulvan concentration. Therefore, the cellulose-ulvan film (C/0.48U) exhibited the lowest light transmittance at 280 nm of only 0.25%, which implied the effectiveness of ulvan in blocking UV-light. Similarly, at the visible light region (400 nm), the light transmission was 40.33% for C film and the incorporation of high concentration of ulvan into the films significantly reduced the light transmission to 19.78% for C/0.48U film. In contrast, the incorporation of ulvan to the cellulose films exhibited non-significant effects on the film opacity at 600 nm (p > 0.05, Table 1). However, at 280 nm the film opacity was significantly increased by increasing ulvan concentration ($p < 0.05$, Table 1), which further confirmed the excellent UV barrier properties of ulvan in the composite films.

Films' water susceptibility

The water solubility (WS) of the biocomposite films were significantly higher in comparison to C film (Table 2). However, increasing ulvan concentration in the developed films showed non-significant effects on the WS values.

The results of the water vapor permeability (WVP) of the developed films are listed in Table 2. Significantly higher WVP values were observed for the biocomposite films in relation to the C film (Table 2). However, increasing of ulvan concentration in the films showed no significant variations in WVP values.
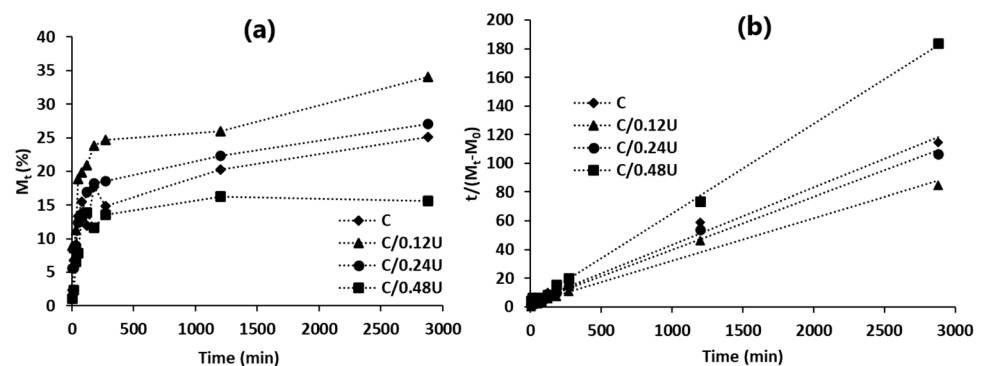
Oxygen permeability (OP)

The OP values exhibited a significant decrease by the incorporation of ulvan to the cellulose films (Table 2), however, increasing ulvan concentration did not induce a significant variation in OP of the composite films.

Moisture sorption

Figure 3 depicts the moisture absorption behavior of the developed films until the equilibrium moisture content is reached. The absorption of moisture was more rapid at the initial stages and low amounts of moisture were adsorbed at longer periods. The coefficients of determination (R^2) of the Peleg's model for all the developed films were very high ($R^2 \geq 0.97$), indicating excellent fitting of the equations to the experimental data (Fig. 3). The Peleg's parameters K_1 and K_2, are shown in Table 3. K_1 is a constant related to the initial moisture adsorption, and low K_1 values are associated with low rate of moisture sorption at the initial stages. While K_2 is a constant related inversely to the maximum water sorption capacity (M_∞). The incorporation of low concentration of ulvan to the cellulose films (C/0.12U) showed significant reduction in the K_1 values in relation to the C film. This reduction was accompanied by higher R_0 values for the C/0.12U film. While C/0.24U and C/0.48U films showed non-significant variation in the K_1 and R_0 values in relation to the C film. In contrast, the biocomposite film with high ulvan concentration (C/0.48U film) exhibited

Table 2 Water solubility (WS), water vapor permeability (WVP), and oxygen permeability (OP) of the developed films from cellulose and ulvan from *U. lactuca*

Film type	WS (%)	WVP ($\times 10^{-10}$ g mm m^{-2} s^{-1} Pa^{-1})	OP ($\times 10^{-3}$ g/100 μm m^2 s)
C	51.75 ± 1.08^a	2.23 ± 0.06^a	13.11 ± 0.87^b
C/0.12U	58.63 ± 0.05^b	2.90 ± 0.18^b	11.55 ± 0.50^a
C/0.24U	56.98 ± 1.34^b	2.86 ± 0.24^b	11.11 ± 0.23^a
C/0.48U	57.305 ± 3.05^b	3.15 ± 0.30^b	10.51 ± 0.05^a

All values are mean ± standard deviation

Different letters in the same column indicate significant difference among different films ($p < 0.05$)

Fig. 3 (**a**) Moisture sorption of the developed films at 25 ℃ and 75% RH as a function of time. (**b**) Application of Peleg's model on moisture sorption data of all the films

high statistically significant K_2 values which implied low moisture absorption capacity at equilibrium (Table 3).

Antioxidant properties

The antioxidant activity of the released active compounds from the cellulose and cellulose-ulvan films was determine after 24 h of contact with different food simulants (water or acetic acid 3%) and the results are listed in Table 4.

The high TAC of the films was registered in water solution, which is attributed to higher solubility of ulvan in water solution. Generally, the biocomposite films exhibited better antioxidant activities in relation to the cellulose film, except for the HRSA in water, the developed films showed non-significant variability. Additionally, the comparison between water and 3% acetic acid as food simulants indicated non-significant variations in the TAC values for the biocomposite films, but in case of FRAP, higher statistically significant values for water than 3% acetic acid was observed. Similarly, the HRSA and ICA values showed negligible variability between water and 3% acetic acid for the biocomposite films except the C/0.24U film and C/0.12U film which exhibited high HRSA and ICA values, respectively in the acid medium.

Thermal gravimetric analysis (TGA)

The thermostability of the developed edible films is depicted in Fig. 4. The thermogravimetric curves allow the study of the thermal degradation of biopolymers and materials. The DTG curves of the developed films show three degradation peaks, the first small peak corresponds to the evaporation of bound water, the second major peak indicates the depolymerization and degradation of cellulose and ulvan, and the third small peak indicates the carbonization of the degradation products. The weight loss at the first degradation stage between 20 and 100 °C was about 12.6, 13.1, 11.1, and 6.6% for C, C/0.12U, C/0.24U, and C/0.48U films, respectively. The temperature at which maximum degradation was obtained was about 238, 240, 226, and 246 °C for C, C/0.12U, C/0.24U, and C/0.48U films, respectively (Fig. 4). It is worth noting that, the temperature of the half weight loss was about 254, 266, 251, and 274 °C for C, C/0.12U, C/0.24U, and C/0.48U film, respectively. The percentages of char (carbonaceous residues) remained after thermal treatment up to 500 °C and the carbonization of the film components are depicted in Fig. 4. The results indicate a concentration dependent increase in the char yield with increasing ulvan concentration in the composite films in relation to the control film.

Table 3 Parameters of Peleg's model at 25 °C for moisture sorption, (K_1 (min %$^{-1}$) is Peleg's rate constant and related to the initial sorption rate (R_0), K_2 (%$^{-1}$) is Peleg's capacity constant and related to the amount of water adsorbed at equilibrium (M_∞)), and the coefficients of determination R^2

Film type	K_1	K_2	R_0	M_∞	R^2
C	3.23 ± 0.26^{bc}	0.040 ± 0.002^a	0.31 ± 0.03^a	25.17 ± 0.98^b	0.99 ± 0.001
C/0.12U	1.86 ± 0.25^a	0.030 ± 0.003^a	0.56 ± 0.07^b	33.71 ± 3.60^c	0.98 ± 0.004
C/0.24U	3.10 ± 0.05^b	0.037 ± 0.001^a	0.32 ± 0.01^a	27.12 ± 0.83^b	0.99 ± 0.001
C/0.48U	4.26 ± 0.36^c	0.063 ± 0.005^b	0.24 ± 0.02^a	15.95 ± 1.14^a	0.97 ± 0.004

All values are mean ± standard deviation

Different letters in the same column indicate significant difference among different films ($p < 0.05$)

Table 4 Total antioxidant capacity (TAC, μg AAEq g^{-1} film), ferric reducing antioxidant power (FRAP, μg AAEq g^{-1} film), hydroxyl radical scavenging activity (HRSA, %) and iron chelating agent (ICA, %) of the developed films from cellulose/ulvan from *U. lactuca*

Film type	TAC		FRAP		HRSA		ICA	
	water	Acetic acid	water	Acetic acid	water	Acetic acid	water	Acetic acid
C	$2.09 \pm 0.13^{a,1}$	$1.53 \pm 0.13^{a,2}$	$0.23 \pm 0.05^{a,1}$	$0.07 \pm 0.02^{a,2}$	$75.32 \pm 0.82^{a,1}$	$39.04 \pm 0.04^{a,2}$	$2.46 \pm 0.7^{a,1}$	$1.28 \pm 0.10^{a,1}$
C/0.12U	$3.53 \pm 0.49^{b,1}$	$3.59 \pm 0.13^{b,1}$	$0.67 \pm 0.01^{b,1}$	$0.24 \pm 0.06^{b,2}$	$73.42 \pm 2.66^{a,1}$	$80.04 \pm 0.51^{b,2}$	$31.87 \pm 0.05^{b,1}$	$56.05 \pm 3.38^{b,2}$
C/0.24U	$4.50 \pm 0.70^{b,1}$	$4.25 \pm 0.44^{bc,1}$	$0.83 \pm 0.07^{b,1}$	$0.25 \pm 0.02^{b,2}$	$78.87 \pm 0.09^{a,1}$	$92.69 \pm 0.88^{c,2}$	$38.36 \pm 3.7^{b,1}$	$50.86 \pm 1.31^{b,2}$
C/0.48U	$6.00 \pm 0.35^{c,1}$	$5.41 \pm 0.75^{c,1}$	$1.18 \pm 0.11^{c,1}$	$0.27 \pm 0.06^{b,2}$	$84.818 \pm 1.45^{a,1}$	$92.02 \pm 0.66^{c,2}$	$52.13 \pm 1.5^{c,1}$	$49.69 \pm 0.92^{b,1}$

All values are mean ± standard deviation

Different letters in the same column indicate significant difference among different films ($p < 0.05$)

Different numbers in the same row indicate significant differences among different solvents ($p < 0.05$)
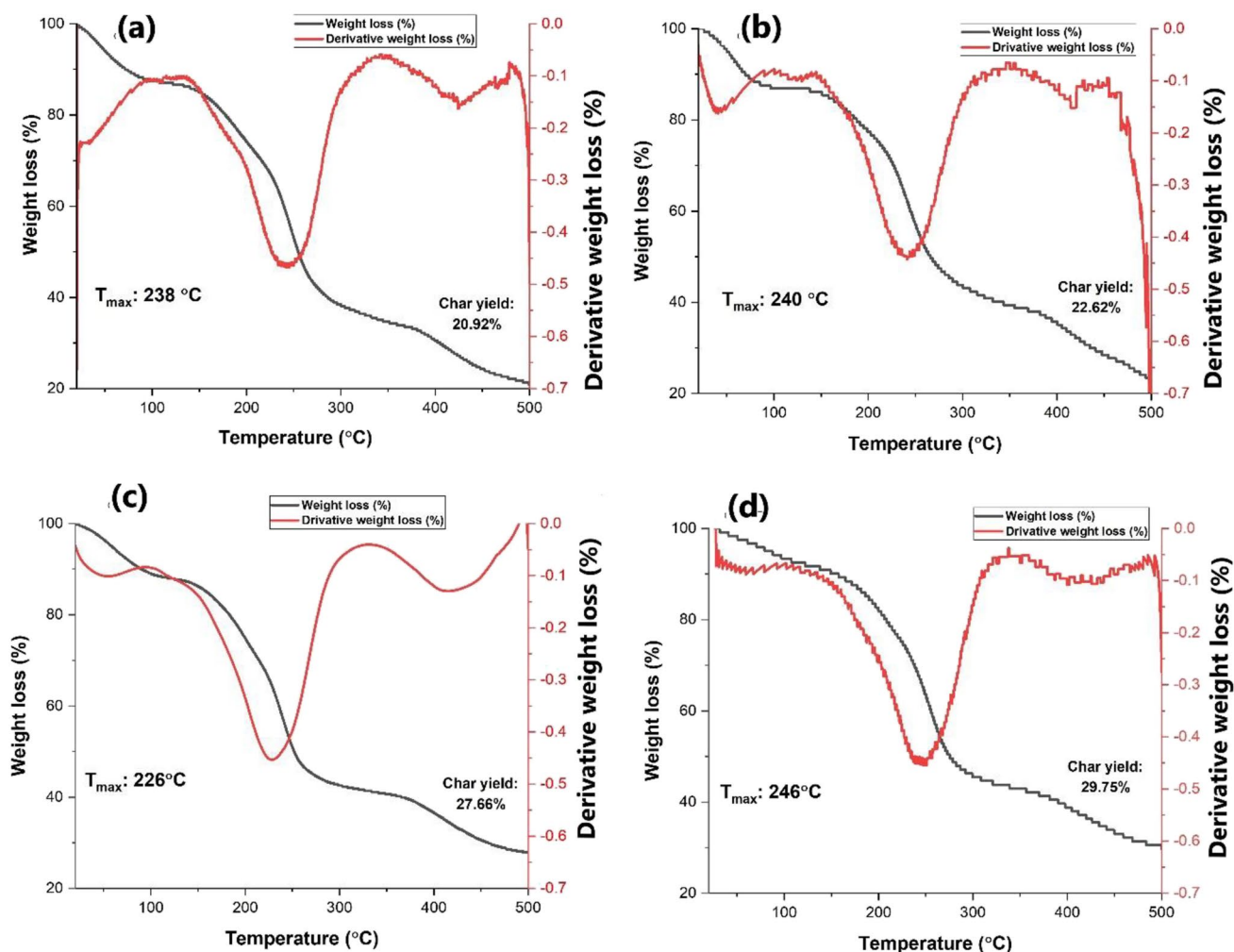
Fig. 4 Thermogravimetric analysis (TGA) curves of the developed films. (**a**) Cellulose, (**b**) Cellulose/0.12 Ulvan, (**c**) Cellulose/0.24 Ulvan, (**d**) Cellulose/0.48 Ulvan

Discussion

Cellulose and ulvan were successfully isolated from the green macroalga *U. lactuca* and were successfully utilized in the development of composite edible films by casting and solvent evaporation process.

The thickness of the developed films increased significantly with the incorporation of ulvan. The incorporation of ulvan can disrupt the dominant hydrogen bonding between cellulose chains to form new cellulose/ulvan interactions as well as it can increase the solid matter contents of the composite films. In general, the film thickness is mainly dependent on the solid matter contents of the film forming solutions (Guidara et al. 2020).

The color and opacity of the films is a crucial property as it can generally influence the visualization and the consumer acceptability of the packaged product. The results indicated

that the developed films have outstanding lightness values as reflected by high $L*$ values. Although ulvan reduced the $L*$ values of the composite films, the results were always higher than 92. This value is higher than those reported for ulvan films plasticized with glycerol or sorbitol (82.43–90.72) (Guidara et al. 2020). Furthermore, the values of $a*$ (<0) and $b*$ (>0) implied that the developed films tended to be green and yellow. However, these parameters exhibited low values which ranged from -2.56 to -2.17 and from 0.9 to 7.33 for $a*$ and $b*$, respectively. The $b*$ values exhibited a concentration dependent increase with increasing ulvan concentration in the biocomposite films indicating that the films were more inclined into the yellow color when the ulvan concentration was increased. Meanwhile, the light transmittance at 280 and 400 nm showed a concentration dependent decrease with increasing ulvan concentration. Similarly, the light absorbance of pure ulvan films plasticized with glycerol or

sorbitol was reported to be less than 5% (Guidara et al. 2019). Accordingly, the biocomposite cellulose/ulvan films can be used for the packaging of different food products with an advantage of high transparency to enable clear vision of the product. Additionally, these films can retard light oxidative deterioration of foods due to their excellent UV light absorbance properties (Gomaa et al. 2018; Guidara et al. 2020).

The high solubility of packaging can be considered as an enhancement for edible coating applications. The water solubility (WS) values of ulvan films are significantly higher in comparison to C film. This can be explained by the smaller molecular weight and the hydrophilic nature of ulvan. Films with high solubility are useful in developing food coatings and food packaging where the food and the film are consumed together, while films with low solubility are usually used for food packaging (Campos et al. 2011). On the other hand, the water vapor transmission by polysaccharide-based films generally occurs through the hydrophilic portion and is related to the ratio of hydrophobic and hydrophilic materials (Wulandari and Warkoyo 2018). Accordingly, the composite films exhibited higher WVP values due to the hydrophilic nature of ulvan. The WS and the WVP showed non-significant effects when ulvan concentration was increased. This may be related to the effects of cellulose and its interactions with ulvan in the composite films. Generally, the composite films exhibited low WVP values ($2.9 – 3.15 \times 10^{-10}$ g mm m^{-2} s^{-1} Pa^{-1}), which is lower than those of films based on pure ulvan ($1.28 – 4.40 \times 10^{-8}$ g mm m^{-2} s^{-1} Pa^{-1}) and carrageenan/ulvan films ($7.82 – 9.96 \times 10^{-8}$ g mm m^{-2} s^{-1} Pa^{-1}) (Ganesan et al. 2018; Guidara et al. 2020).

Oxygen permeability is the ability of oxygen gas to cross the film under certain circumstances and it is useful for estimating the shelf life of packaged products. The OP values exhibited a significant decrease by incorporating ulvan to the cellulose films. This observation may be attributed to the hydrogen bonds between cellulose and ulvan as proved by FT-IR analysis which enhanced the compactness of the film and resulted in reducing the channels within the film matrix. Additionally, these strong intermolecular interactions could contribute to the thermal stability of the films. Refering to the literature, the thermal degradation of polysaccharides occurs in four distinct steps. The first step includes the desorption of physically bound water, followed by a second step of dehydration. During the third step, polysaccharides are depolymerized and structural bonds such as C-O and C–C begins to degrade resulting in the evolution of CO, CO_2 and H_2O. The last step is accompanied by the formation of polynuclear aromatic and graphitic carbon structures (Yaich et al. 2017). The existence of ulvan decreased the rate of water weight loss at temperatures up to 100 ºC as well as it reduced the water content of the films. Furthermore, the incorporation of high concentration of ulvan (C/0.48U film) significantly enhanced the thermal stability of the composite film compared to the control (C film).

On the other hand, active coatings and films with antioxidant properties can improve the stability of fresh foods and extend their shelf life. The antioxidant capacity of ulvan have been proved in previous studies (Li et al. 2018; Guidara et al. 2019). In the present study, the incorporation of ulvan to cellulose films enhanced its antioxidant properties. Similarly, Ganesan et al. (2018) and Guidara et al. (2019) demonstrated that ulvan-based films have strong antioxidant properties. Futhermore, it has been reported that the reducing power and chelating activity of ulvan is attributed to its glucuronic acid, hydroxyl groups and sulfate groups (Qi et al. 2006). In the present study, FRAP of ulvan films was significantly higher in water than 3% acetic acid as food simulants. Guidara et al. (2019) demonstrated that DPPH activity of ulvan is strongly dependent on the pH of the solution. In acetic acid solution the carboxylate groups of ulvan were protonated and thus its ferric reducing potential was reduced. Similarly, Gomaa et al. (2018) reported that alginate/fucoidan composite films had an enhancement of FRAP in aqueous solutions compared to acidic food simulants. Based on the present results, the developed composite films can play a significant role in effectively chelating metal ion and scavenging free radicals; thus, increasing the stability of the packaged food product by finishing the radical chain reaction.

Conclusion

Composite films with high antioxidant properties were prepared by incorporating different concentrations of ulvan into cellulose. These polysaccharides were extracted from the same biomass of *U. lactuca* which supports the seaweed biorefinery industry. The results showed that the incorporation of different ulvan concentrations into the cellulose-based films increased thickness, WVP and WS while, decreased OP of the composite films. The composite films were also characterized by enhanced barrier properties against UV and visible light. In addition, these films exhibited high antioxidant properties, which is mainly affected by the type of food simulant. Based on the results, C/0.48U film showed promising thermal, barrier, and antioxidant properties which supports its potential application in food packaging and coating.

Data availability The datasets used and/or analyzed during the current study are available from the corresponding author on reasonable request.

Declarations

References

Albalasmeh AA, Berhe AA, Ghezzehei TA (2013) A new method for rapid determination of carbohydrate and total carbon concentrations using UV spectrophotometry. Carbohydr Polym 97:253–261

Bhadja P, Tan C-Y, Ouyang J-M, Yu K (2016) Repair effect of seaweed polysaccharides with different contents of sulfate group and molecular weights on damaged HK-2 Cells. Polymers (Basel) 8:188

Bhattacharya D, Kandeepan G (2017) Selection of biopolymers to develop a biodegradable and edible film for packaging of luncheon chicken meat slices. Asian J Dairy Food Res 36:67–71

Bitter T (1962) A modified uronic acid carbazole reaction. Anal Biochem 4:330–334

Bogolitsyn K, Parshina A, Aleshina L (2020) Structural features of brown algae cellulose. Cellulose 27:9787–9800

Campos CA, Gerschenson LN, Flores SK (2011) Development of edible films and coatings with antimicrobial activity. Food Bioprocess Technol 4:849–875

El Achaby M, Kassab Z, Aboulkas A, Gaillard C, Barakat A (2018) Reuse of red algae waste for the production of cellulose nanocrystals and its application in polymer nanocomposites. Int J Biol Macromol 106:681–691

Fernando IPS, Sanjeewa KKA, Samarakoon KW, Lee WW, Kim H-S, Kim E-A, Gunasekara UKDSS, Abeytunga DTU, Nanayakkara C, de Silva ED, Lee H-S, Jeon Y-J (2017) FTIR characterization and antioxidant activity of water soluble crude polysaccharides of Sri Lankan marine algae. Algae 32:75–86

Ferreira ICFR, Baptista P, Vilas-Boas M, Barros L (2007) Free-radical scavenging capacity and reducing power of wild edible mushrooms from northeast Portugal: Individual cap and stipe activity. Food Chem 100:1511–1516

Galus S, Lenart A (2013) Development and characterization of composite edible films based on sodium alginate and pectin. J Food Eng 115:459–465

Ganesan AR, Shanmugam M, Bhat R (2018) Producing novel edible films from semi refined carrageenan (SRC) and ulvan polysaccharides for potential food applications. Int J Biol Macromol 112:1164–1170

Gomaa M, Fawzy MA, Hifney AF, Abdel-Gawad KM (2018) Use of the brown seaweed *Sargassum latifolium* in the design of alginate-fucoidan based films with natural antioxidant properties and kinetic modeling of moisture sorption and polyphenolic release. Food Hydrocoll 82:64–72

Gomaa M, Al-Badaani AA, Hifney AF, Adam MS (2021) Industrial optimization of alkaline and bleaching conditions for cellulose extraction from the marine seaweed *Ulva lactuca*. J Appl Phycol 33:4039–4103

Guidara M, Yaich H, Richel A, Blecker C, Boufi S, Attia H, Garna H (2019) Effects of extraction procedures and plasticizer concentration on the optical, thermal, structural and antioxidant properties of novel ulvan films. Int J Biol Macromol 135:647–658

Guidara M, Yaich H, Benelhadj S, Adjouman YD, Richel A, Blecker C, Sindic M, Boufi S, Attia H, Garna H (2020) Smart ulvan films responsive to stimuli of plasticizer and extraction condition in physico-chemical, optical, barrier and mechanical properties. Int J Biol Macromol 150:714–726

Hung Y-HR, Chen G-W, Pan C-L, Lin H-TV (2021) Production of ulvan oligosaccharides with antioxidant and angiotensin-converting enzyme-inhibitory activities by microbial enzymatic hydrolysis. Fermentation 7:160

Hussein MH, Hamouda RA, El. El-Naggar N, Karim-Eldeen MA (2015) Characterization, antioxidant potentiality and biological activities of the polysaccharide ulvan extracted from the marine macroalga *Ulva* spp. J Agric Chem Biotechnol 6:373–392

Jmel MA, Ben MG, Marzouki MN, Mathlouthi M, Smaali I (2016) Physico-chemical characterization and enzymatic functionalization of *Enteromorpha* sp. cellulose. Carbohydr Polym 135:274–279

Jost V, Kobsik K, Schmid M, Noller K (2014) Influence of plasticiser on the barrier, mechanical and grease resistance properties of alginate cast films. Carbohydr Polym 110:309–319

Kidgell JT, Magnusson M, de Nys R, Glasson CRK (2019) Ulvan: A systematic review of extraction, composition and function. Algal Res 39:101422

Lee CM, Kubicki JD, Fan B et al (2015) Hydrogen-bonding network and OH stretch vibration of cellulose: Comparison of computational modeling with polarized IR and SFG spectra. J Phys Chem B 119:15138–15149

Li W, Jiang N, Li B, Wan M, Chang X, Liu H, Zhang L, Yin S, Qi H, Liu S (2018) Antioxidant activity of purified ulvan in hyperlipidemic mice. Int J Biol Macromol 113:971–975

Lister E, Wilson P (2001) Measurement of total phenolics and ABTS assay for antioxidant activity (personal communication). Crop Res Institute, Lincoln

Lowry OH, Rosebrough NJ, Farr AL, Randall RJ (1951) Protein measurement with the Folin phenol reagent. J Biol Chem 193:265–275

Peleg M (1988) An empirical model for the description of moisture sorption curves. J Food Sci 53:1216–1217

Pirsa S, Farshchi E, Roufegarinejad L (2020) Antioxidant/antimicrobial film based on carboxymethyl cellulose/gelatin/TiO_2–Ag nano-composite. J Polym Environ 28:3154–3163

Prabhu M, Chemodanov A, Gottlieb R, Kazir M, Nahor O, Gozin M, Israel A, Livney YD, Golberg A (2019) Starch from the sea: the green macroalga *Ulva ohnoi* as a potential source for sustainable starch production in the marine biorefinery. Algal Res 37:215–227

Prieto P, Pineda M, Aguilar M (1999) Spectrophotometric quantitation of antioxidant capacity through the formation of a phosphomolybdenum complex: specific application to the determination of vitamin E. Anal Biochem 269:337–341

Puntel RL, Nogueira CW, Rocha JBT (2005) Krebs cycle intermediates modulate thiobarbituric acid reactive species (TBARS) production in rat brain in vitro. Neurochem Res 30:225–235

Qi H, Zhang Q, Zhao T, Hu R, Zhang K, Li Z (2006) In vitro antioxidant activity of acetylated and benzoylated derivatives of polysaccharide extracted from *Ulva pertusa* (Chlorophyta). Bioorg Med Chem Lett 16:2441–2445

Qi H, Chang C, Zhang L (2008) Effects of temperature and molecular weight on dissolution of cellulose in NaOH/urea aqueous solution. Cellulose 15:779–787

Razavi SMA, Amini AM, Zahedi Y (2015) Characterisation of a new biodegradable edible film based on sage seed gum: Influence of plasticiser type and concentration. Food Hydrocoll 43:290–298

Schwanninger M, Rodrigues JC, Pereira H, Hinterstoisser B (2004) Effects of short-time vibratory ball milling on the shape of FT-IR spectra of wood and cellulose. Vib Spectrosc 36:23–40

Sucaldito MR, Camacho DH (2017) Characteristics of unique HBr-hydrolyzed cellulose nanocrystals from freshwater green algae (*Cladophora rupestris*) and its reinforcement in starch-based film. Carbohydr Polym 169:315–323

Syarifuddin A, Hamsiohan P, Bilang M (2019) Characterization of edible film from dangke whey/pectin, beeswax, and butter aroma. AIP Conf Proc 2155:020021

Tavassoli-Kafrani E, Shekarchizadeh H, Masoudpour-Behabadi M (2016) Development of edible films and coatings from alginates and carrageenans. Carbohydr Polym 137:360–374

Valizadeh S, Naseri M, Babaei S, Hosseini SMH, Imani A (2019) Development of bioactive composite films from chitosan and carboxymethyl cellulose using glutaraldehyde, cinnamon essential oil and oleic acid. Int J Biol Macromol 134:604–612

Wulandari Y, Warkoyo NH (2018) Characterization of edible film from starch of taro (*Colocasia esculenta* (L.) Schott) with addition of chitosan on dodol substituted seaweed (*Eucheuma cottonii* L.). Food Technol Halal Sci J 1:22–32

Xie Y, Pan Y, Cai P (2022) Hydroxyl crosslinking reinforced bagasse cellulose/polyvinyl alcohol composite films as biodegradable packaging. Ind Crops Prod 176:114381

Yaich H, Amira AB, Abbes F, Bouaziz M, Besbes S, Richel A, Blecker C, Attia H, Garna H (2017) Effect of extraction procedures on structural, thermal and antioxidant properties of ulvan from *Ulva lactuca* collected in Monastir coast. Int J Biol Macromol 105:1430–1439

Zanchetta E, Damergi E, Patel B, Borgmeyer T, Pick H, Pulgarin A, Ludwig C (2021) Algal cellulose, production and potential use in plastics: Challenges and opportunities. Algal Res 56:102288

Zhang P, Zhao Y, Shi Q (2016) Characterization of a novel edible film based on gum ghatti: Effect of plasticizer type and concentration. Carbohydr Polym 153:345–355

Zhong X-K, Jin X, Lai F-Y, Lin Q-S, Jiang J-G (2010) Chemical analysis and antioxidant activities in vitro of polysaccharide extracted from *Opuntia ficus indica* Mill. cultivated in China. Carbohydr Polym 82:722–727

Zhou J, Zhang L, Cai J (2004) Behavior of cellulose in NaOH/urea aqueous solution characterized by light scattering and viscometry. J Polym Sci B 42:347–353